Finite-Difference Model Predictions of the Drastic Retreat of Columbia Glacier, Alaska

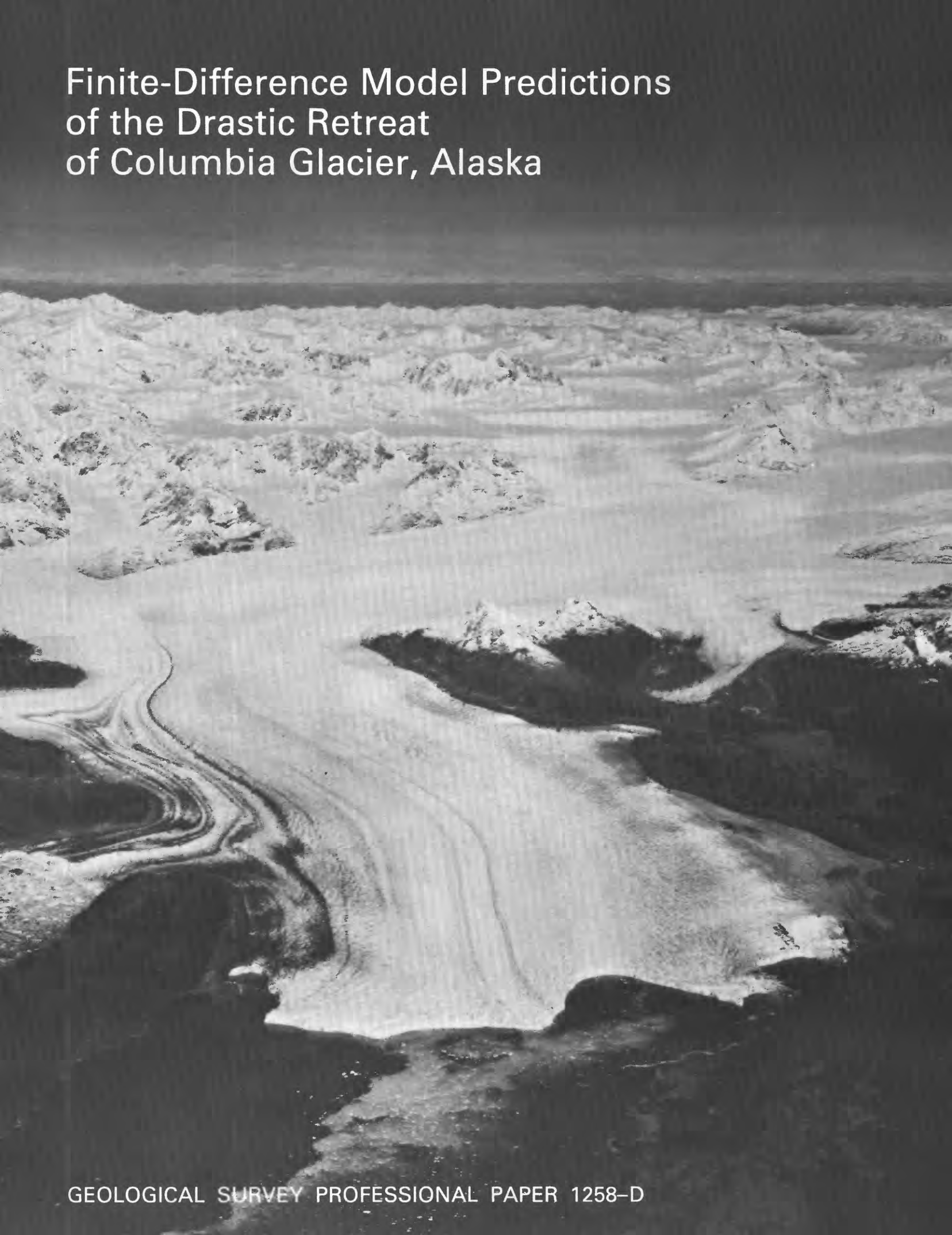

GEOLOGICAL SURVEY PROFESSIONAL PAPER 1258–D

Finite-Difference Model Predictions of the Drastic Retreat of Columbia Glacier, Alaska

By R. A. Bindschadler and L. A. Rasmussen

STUDIES OF COLUMBIA GLACIER, ALASKA

GEOLOGICAL SURVEY PROFESSIONAL PAPER 1258-D

Discussion of a one-dimensional dynamic model developed to predict the retreat and the iceberg discharge from a large iceberg-calving glacier

UNITED STATES GOVERNMENT PRINTING OFFICE, WASHINGTON:1983

UNITED STATES DEPARTMENT OF THE INTERIOR

JAMES G. WATT, *Secretary*

GEOLOGICAL SURVEY

Dallas L. Peck, ***Director***

Library of Congress Cataloging in Publication Data
Bindschadler, R. A. (Robert A.)
Finite-difference model predictions of the drastic retreat of Columbia Glacier, Alaska.
(Studies of Columbia Glacier, Alaska) (Geological Survey professional paper ; 1258-D)
"Discussion of a one-dimensional dynamic model developed to predict the retreat and the iceberg discharge from a large iceberg-calving glacier."
Bibliography: p.
Supt. of Doc. no.: I 19.16:1258-D
1. Columbia Glacier (Alaska)—Mathematical models. 2. Finite differences. I. Rasmussen, L. A. II. Title. III. Series. IV. Series: Geological Survey professional paper ; 1258-D.
GB2425.A4B56 1983 551.3'12'097983 83-600208

For sale by the Distribution Branch, U.S. Geological Survey,
604 South Pickett Street, Alexandria, VA 22304

CONTENTS

ILLUSTRATIONS

TABLE

SYMBOLS AND ABBREVIATIONS

Symbol	Name	Unit
A	Coefficient in ice-flow law	$\mathrm{bar}^{-n}\ \mathrm{a}^{-1}$
a	Year	
$\dot{b}$	Mass balance (ice equivalent)	$\mathrm{m\ a}^{-1}$
c	Coefficient in calving law (water law)	a^{-1}
c'	Coefficient in calving law (ice law)	a^{-1}
f	Velocity shape factor	dimensionless
f^*	Flux shape factor	dimensionless
g	Gravitational acceleration	$\mathrm{m\ s}^{-2}$
h_w	Water depth at terminus	m
H	Ice thickness (vertical)	m
H^*	Ice thickness at terminus	m
i	Gridpoint index	dimensionless
m	Time step index	dimensionless
n	Exponent in ice-flow law	dimensionless
P	Coefficient of transverse channel shape	$\mathrm{m}^{1/2}$
Q	Volume flux	$\mathrm{m}^3\ \mathrm{a}^{-1}$
$\widetilde{Q}$	Calving flux	$\mathrm{m}^3\ \mathrm{a}^{-1}$
R	Coefficient of transverse channel shape	dimensionless
S	Channel cross-section area	m^2
t	Time	a
$\triangle t$	Time step	a

Symbol	Name	Unit
U	Deformation velocity	$\mathrm{m\ a}^{-1}$
V	Total velocity	$\mathrm{m\ a}^{-1}$
$\widetilde{V}$	Calving velocity	$\mathrm{m\ a}^{-1}$
W	Channel width	m
x	Longitudinal coordiante	m
X^*	Terminus position	m
Y	Bed elevation	m
α	Surface slope	dimensionless
β	Thickness gradient	dimensionless
δ	Advance of terminus	m
$\dot{\epsilon}$	Strain rate	a^{-1}
ϕ	Weighting factor for effective stress	dimensionless
λ	Ratio of sliding to total velocity	dimensionless
ϱ	Density of ice	$\mathrm{kg\ m}^{-3}$
ϱ_w	Density of water	$\mathrm{kg\ m}^{-3}$
τ	Effective base shear stress	$\mathrm{N\ m}^{-2}$
τ'	Effective deviatoric stress	$\mathrm{N\ m}^{-2}$
τ^*	Base shear stress	$\mathrm{N\ m}^{-2}$
$\overline{\tau^*}$	Average base shear stress	$\mathrm{N\ m}^{-2}$
θ	Weighting factor in calving law	dimensionless

STUDIES OF COLUMBIA GLACIER, ALASKA

FINITE-DIFFERENCE MODEL PREDICTIONS OF THE DRASTIC RETREAT OF COLUMBIA GLACIER, ALASKA

By R. A. BINDSCHADLER[1] and L. A. RASMUSSEN

ABSTRACT

A finite-difference model of Columbia Glacier is used to study the possible retreat of the terminus. The model calculates the glacier motion from the glacier geometry via relationships of glacier dynamics and updates the glacier geometry in time increments via the continuity equation and a prescribed mass balance function. The sliding velocity is assumed to have the same functional relationship to glacier geometry as does the velocity due to deformation. Values of model parameters are fit to Columbia Glacier data gathered during the 1977–78 mass balance year. Approach to flotation of the terminus is implied by the model as the cause of the predicted rapid retreat and is a direct consequence of the rapid thinning observed at the terminus. Alternative schemes are examined to treat a floating terminus. In all cases, a rapid retreat eventually occurs.

INTRODUCTION

Columbia Glacier is one of the larger Alaska glaciers. Located a few kilometers west of Valdez, the glacier covers a 1,100-km^2 area with the longest tributary stretching more than 66 km (fig. 1). Many large tributaries coalesce to form the lower trunk of the glacier, which fills a deep fiord and ends in a calving terminus towering 90 m above sea level at the head of Columbia Bay. Although the altitude of the bed beneath the glacier reaches depths of more than 400 m below sea level, it average less than 100 m below sea level at the terminus. This is because the terminus rests on a high ridge of material deposited by the glacier itself as it advanced into what was once a larger Columbia Bay (Post, 1975). Similar shoal features are found at the outlets of other glacially scoured fiords in Alaska (Post, 1980a–f), but Columbia Glacier is unique as the only glacier which still extends out to its neoglacial shoal.

[1]Code 912.1, Ice Station, Goddard Laboratory for Atmospheric Sciences, NASA/Goddard Space Flight Center, Greenbelt, MD 20771.

Considerable evidence now suggests that the terminus of Columbia Glacier, in near equilibrium since the first recorded observation in 1794, is on the verge of a rapid and drastic retreat from its shoal (Post, 1975; Sikonia and Post, 1979). An intensive study of Columbia Glacier, begun in 1977 by the U.S. Geological Survey, has documented an accelerated rate of thinning in the terminus region and a trend of increasingly larger embayments being formed as an ever greater fraction of the terminus retreats from the crest of the shoal each summer. These partial retreats are believed to be precursory to the drastic, wholesale retreat soon to commence when the small fraction of terminus resting in shallow water can no longer prevent irreversible embayment growth. Observations of calving glaciers (grounded glaciers which terminate in tidal waters and discharge icebergs) have established that stable or nearly stable terminii occur at water depths of less than 80 m and that, when terminii have had to retreat through deeper waters, the retreats have been very fast (Meier and others, 1980).

A direct consequence of a rapid retreat is an increased flux of icebergs. In the case of Columbia Glacier, the presence of icebergs in Columbia Bay is a concern owing to the proximity of the shipping lanes in Valdez Arm, which is less than 20 km from the terminus (fig. 1), used by tankers transporting Alaska pipeline oil stored in nearby Valdez. Even at current ice discharge rates, small icebergs drift into the shipping lanes (Kollmeyer and others, 1977). At increased calving rates, more numerous, larger icebergs might create a hazard to shipping.

Because of this potential hazard, the U.S. Geological Survey initiated its investigation of Columbia Glacier (Meier and others, 1978). Details of each phase of this study are being published as a series of scientific papers, of which this is one. Those already published discuss the relation between iceberg calving and water

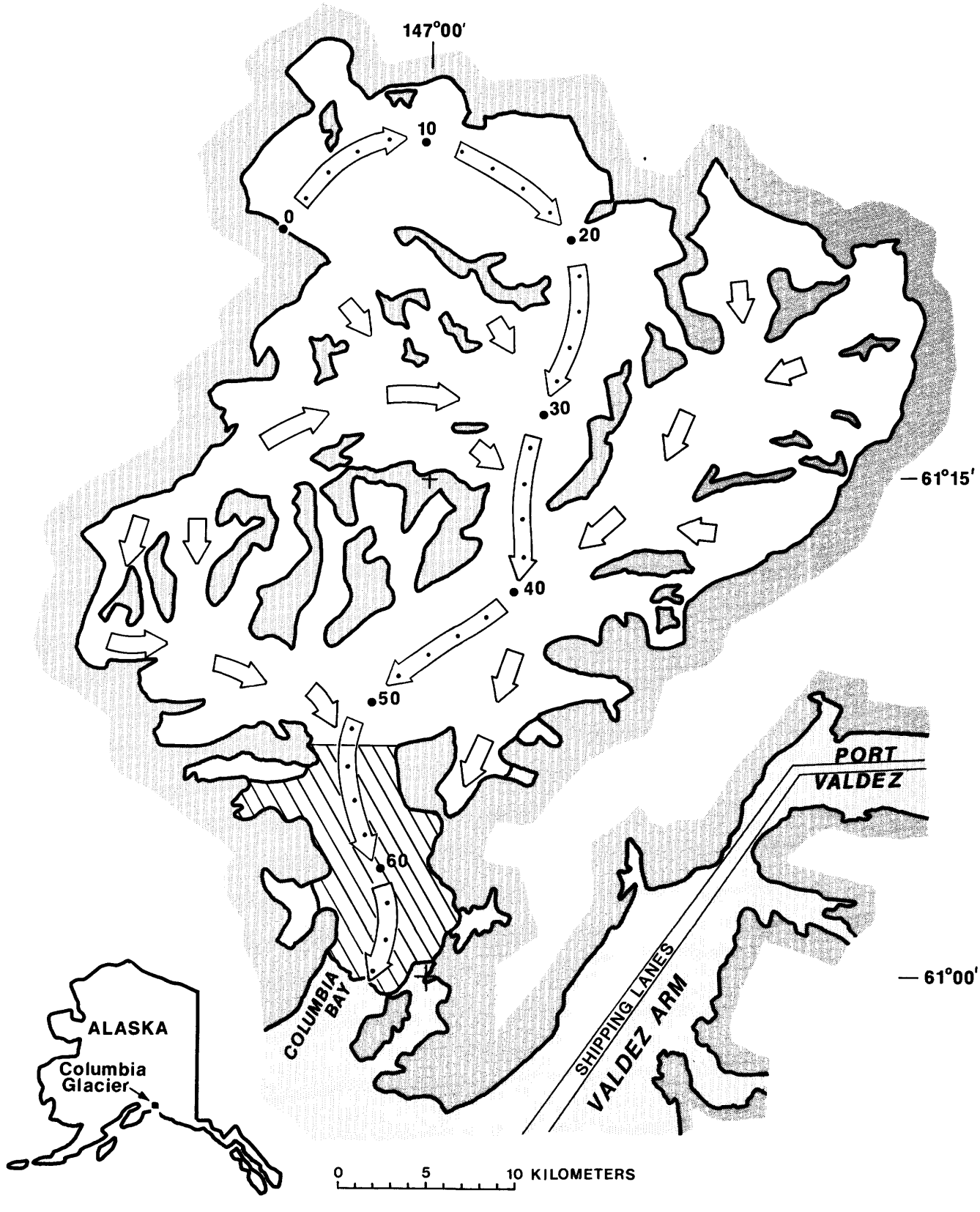

FIGURE 1. Map of Columbia Glacier. Arrows indicate direction of ice flow. Largest tributary is marked every 2 km from ice divide to terminus. Modeled region, beginning at the 53-km mark, is hachured.

depth (Brown and others, 1982); the adjustment and interpolation of point data (Sikonia, 1983); a finite-element model of the lower glacier (Sikonia, 1982); and a continuity-equation model of the lower glacier (Rasmussen and Meier, 1982).

This paper discusses the results of applying a finite-difference numerical model of glacier flow to the lower reach of Columbia Glacier (fig. 1) to predict its future behavior. Modeling a tidewater glacier such as Columbia Glacier presents a new and challenging problem in glacier dynamics. A major aspect of this program is the time-dependent behavior of the terminus. This modeling is also important because of the potential hazard of discharged icebergs to shipping. The parameterization of calving was an important element of each model (this finite-difference model as well as the continuity and finite-element models referenced above) but was limited by knowledge of the calving process and its controls. Thus, any model is restricted by gaps in our understanding and can only predict a range of possible future behaviors. Available data help reduce the range of the predictions, but further refinements can only result from future observations. Nevertheless, it is encouraging that, although each of the three numerical models took different approaches and made different assumptions, the general results were similar.

ACKNOWLEDGMENTS

The authors are grateful to Dr. R. H. Thomas and Dr. E. D. Waddington for carefully reviewing the original version of the manuscript and for making numerous constructive suggestions.

PREVIOUS MODELING OF COLUMBIA GLACIER

The continuity model of Rasmussen and Meier (1982) incorporated a minimum of glacier dynamics into the predictions of terminus retreat. By requiring mass conservation, the time intervals between a set of sequential elevation profiles were calculated. The series of profiles was interpolated between the measured elevation profile existing in 1978 and an hypothesized elevation profile corresponding to a 14-km retreat of the terminus. The model was one-dimensional, simulating the retreat along a central flowline, and was independent of any transverse variations in any of the parameters. The calving flux in this model was specified to depend linearly on the water depth at the terminus. The details of this relationship are discussed in a later section. The results of this continuity model predicted that the terminus will begin a drastic retreat in the 1980's. The speed of the predicted retreat depended on the value of a parameter in the calving term but was on the order of 4 km a^{-1}, with a maximum calving flux of about 10 km^3 a^{-1} (compared with about 1 km^3 a^{-1} in 1978).

The finite-element model of Sikonia (1982) analyzed the flow of a vertical section along a central flowline over the lower 14 km of the glacier. A thin layer of elements with a very low viscosity at the base of the glacier was used to simulate basal sliding. The calving flux in this model was related to the ice thickness at the terminus unsupported by buoyancy and included a superimposed seasonal variation due to the apparent dependence of calving on freshwater runoff. The results of this modeling were extremely sensitive to the precise values of the calving law parameters; seemingly minor variations in these parameters caused variations ranging from no retreat to drastic retreat before 1980.

FINITE-DIFFERENCE MODEL

The finite-difference model, which is applied here to Columbia Glacier, was originally developed as a general glacier model capable of simulating the dynamics of valley glaciers whose motion is predominantly due to internal deformation of the ice. It was first applied to predict the behavior of a surge-type glacier during the quiescent phase of motion (Bindschadler, 1982). The model is described in Bindschadler (1982), and additional detail can be found in Bindschadler (1978); what will be presented here is a summary of the approach used and the assumptions made in applying this model to Columbia Glacier.

PARAMETERIZATION OF GLACIER GEOMETRY

The model is one-dimensional; the profile of glacier depth, $H(x)$, along a central flowline (x axis) is the principal dependent variable. The transverse channel cross section is specified by the equation,

$$W(x,z)=P(x)z^{1/2}+R(x)z, \quad (1)$$

relating the channel width, W, to the height, z, above the glacier bed, and describing, the shape of the channel, P and R. Equation 1 represents a linear combination of channels with either a parabolic or V-shaped cross section, the shapes most common for mountain glaciers. The cross section area is obtained by integrating equation 1 over the depth:

$$S(x)=\tfrac{2}{3}P(x)[H(x)]^{3/2}+\tfrac{1}{2}R(x)[H(x)]^2. \quad (2)$$

For a known set of widths, cross-section areas and depths, equations 1 and 2 can be used to determine the values of P and R at each x. Once the parameters are determined and the bed elevation, $Y(x)$, is specified, changes in the geometry of the glacier depend only on changes in $H(x)$. Thus, in strict mathematical terms, the model is one-dimensional; however, equations 1 and 2 parameterize additional dimensions which affect the dynamic behavior of the glacier. The effect of a channel with sloping sides is to slow the speed of the glacier's response to changing conditions (Bindschadler, 1978, p. 127).

CONTINUITY EQUATION

For each time step, the ice motion is calculated from the glacier geometry and is used to update the depth profile through the vertically integrated continuity equation,

$$\frac{\partial S(x)}{\partial t}+\frac{\partial Q(x)}{\partial x}=\dot{b}(x)W(x), \tag{3}$$

where $Q(x)$ is the volume flux along the x-axis, $\dot{b}(x)$ is the mass balance, $W(x)$ is the surface width, and t represents time. Each of the variables in equation 3 must either be specified or calculated from the geometry.

GLACIER DYNAMICS

BASE SHEAR STRESS

Gravitational forces create stresses within the ice which cause it to deform. This deformational motion of the ice is one component of the ice velocity; the other is basal sliding and is discussed later. If it is assumed that the top and bottom surfaces of the glacier are parallel, that there are no longitudinal stress gradients, and that the glacier is infinitely wide, then the flow is laminar and the shear stress at the glacier bed is

$$\tau^*(x)=\varrho g H(x)\cos\alpha(x)\sin\alpha(x), \tag{4}$$

where ϱ is the ice density, g is the gravitational acceleration, α is the surface slope, and $H(x)\cos\alpha(x)$ is the surface normal depth.

On Columbia Glacier, the surface and bed are nearly parallel, but longitudinal stresses vary along the width, and the channel is not infinitely wide. However, equation 4 can be modified to partially account for these effects. Longitudinal stress variations occur whenever the longitudinal gradient of velocity is not constant. By averaging the surface slope in equation 4 over distances of 10 to 20 times the glacier depth, the effects of longitudinal stress gradients are greatly smoothed, permitting a more accurate calculation of the longitudinal velocity profile (Budd, 1970; Meier and others, 1974). In this model, the entire right-hand side of equation 4 will be averaged over these distances, but, because the variation of $\alpha(x)$ is much larger than the variation in $H(x)$, the differences between the two averaging methods are small. These averaged base stresses are denoted $\overline{\tau^*}$, and the modified base shear stress is

$$\overline{\tau^*}(x)=\varrho g\overline{H(x)\cos\alpha(x)\sin\alpha(x)}. \tag{5}$$

A second modification to the basal shear stress takes account of the friction of the moving ice against the valley walls, which causes additional shear within the ice. The magnitude of this shear is less than at the centerline where the maximum depth is assumed to occur. Thus, the mean shear stress in the ice is some fraction, $f\leq 1$, of the shear stress in equation 5. Nye (1965) has calculated this fraction (referred to here as the "velocity shape factor") for various channel shapes. His calculations show that f is insensitive to changes in ice depth for a given cross-section shape.

A final modification to equation 5 was required to preserve numerical stability in the finite-difference solution (a discussion of the problem of numerical stability in glacier modeling can be found in Waddington, 1981, Section 2.2.4). Values of $\overline{\tau^*}$ were combined with unaveraged τ^*; the linear combination of these two stresses formed an "effective" average base stress,

$$\tau(x)=f(x)[\phi\overline{\tau^*}(x)+(1-\phi)\tau^*(x)], \tag{6}$$

where ϕ is a positive weighting factor, less than unity. For values of ϕ close to unity, this final modification has little effect on the overall dynamics of the glacier. A detailed study of the numerical stability showed that ϕ depended slightly on the averaging distance in $\overline{\tau^*}$ but that $\phi=0.8$ always ensured numerical stability (Bindschadler, 1978, Section 5.6.4).

DEFORMATION VELOCITY

The rate of deformation in the ice that results from an applied stress is usually expressed as the following nonlinear flow law:

$$\dot{\epsilon}=A(\tau')^n \tag{7}$$

(Nye, 1957), where $\dot{\epsilon}$ is the effective strain rate, τ' is the effective deviatoric stress, and n and A are empirically determined parameters. Using equation 6 and integrating over the depth, the ice deformation velocity at

the glacier surface due to the effective average shear stress, τ, is

$$U(x)=\frac{2A}{n+1}[\tau(x)]^n H(x)\cos\alpha(x). \quad (8)$$

SLIDING VELOCITY

The second component of ice velocity is the sliding velocity. Unfortunately, the understanding of this process is very poor. Expansive theoretical developments on this subject fall far short of being able to predict sliding velocity from glacier geometry (Meier, 1968). Field measurements of Columbia Glacier show that sliding is a major fraction of the velocity near the terminus (W. G. Sikonia, written commun., 1979); therefore, some parameterization of sliding was required for the model. In lieu of using complex schemes of sliding with no sound physical basis, it was felt most expedient to use a simple parameterization which includes the known important variables of sliding. The most important variables controlling sliding are basal shear stress, bed roughness, and either subglacial water pressure (Bindschadler, 1983) or subglacial cavity growth (Iken, 1981). For the model, bed roughness, water pressure, and the growth rate of subglacial cavities were taken as constant in time at each point in space, but changes in the basal shear stress were calculated from equations 4, 5, and 6. The simplest conversion of the base shear stress to sliding velocity is to assume the same form of relationship as equation 8, including the same value for the exponent. There is additional justification for assuming a nonlinear sliding law; various theoreticians (Kamb, 1970; Weertman, 1964; Lliboutry, 1968; Morland, 1976a, b) have derived such relationships, but there is some disagreement on whether the value of the stress exponent is the same n as in equation 7. This assumption is equivalent to postulating that the ratio of the sliding velocity to total surface velocity is a constant at each point in space. Thus, a parameter λ is defined as

$$\lambda(x)=\frac{V(x)-U(x)}{V(x)}, \quad (9)$$

where $V(x)$ is the total surface velocity. Values of $\lambda(x)$ were determined from the field data by considering the annual variation of velocity and assuming the winter minimum velocity to be due entirely to deformational motion.

VOLUME FLUX

Finally, the velocity must be converted to a volume flux. Because the surface velocity at the channel center is the maximum velocity over the entire cross section, a final parameter, the "flux shape factor," $f^* \le 1$, is defined as the ratio of the deformation velocity averaged over the entire cross-section area, S, to the maxinum deformation velocity, U (eq 8). By assuming that the sliding component of motion is constant over the ice-rock interface in the section, the volume flux can be written

$$Q(x)=[f^*(x)U(x)+V(x)-U(x)]S(x). \quad (10)$$

As with the velocity shape factor, the flux shape factor is not sensitive to thickness changes (Nye, 1965); once the values are determined for f and f^*, they are held constant in time.

FINITE-DIFFERENCE EQUATIONS

In the finite-difference method, the terms of the continuity equation (eq 3) must be represented by finite differences on a discrete grid. The gridpoints occur at x_i $(1 \le i \le p)$; depth, H_i; bed elevation, Y_i; cross-section area, S_i; channel width, W_i; and mass balance, $\dot{b}_i$ are either specified or calculated at each x_i, and the volume fluxes, $Q_{i+1/2}$, are calculated at the grid midpoints, $x_{i+1/2}$ (fig. 2). Thus, the finite-difference form of the continuity equation is

$$\frac{S_i^{m+1}-S_i^m}{t^{m+1}-t^m}+\frac{Q_{i+1/2}^{m+1/2}-Q_{i-1/2}^{m+1/2}}{\frac{1}{2}(x_{x+1}-x_{i-1})}=\dot{b}_i\, W_i, \quad (11)$$

where $Q_{i+1/2}^{m+1/2}=\frac{1}{2}(Q_{i+1/2}^{m+1}+Q_{i+1/2}^{m})$, and superscripts refer to the time step index m or $(m+1)$. (12)

Equations 11 and 12 are referred to as the Crank-Nicholson finite-difference scheme, where the term $Q_{i+1/2}^{m+1/2}$ is the average volume flux over the time step (McCracken and Dorn, 1964). The finite difference forms of the ancillary equations are

$$W_i=P_i\, H_i^{1/2}+R_i\, H_i \quad (13)$$

$$S_i=\tfrac{2}{3}P_i\, H_i^{3/2}+\tfrac{1}{2}R_i\, H_i^2 \quad (14)$$

$$Q_{i+1/2}=\left[f^*_{i+1/2}+\frac{\lambda_{i+1/2}}{1-\lambda_{i+1/2}}\right]U_{i+1/2}\left(\frac{S_{i+1}+S_i}{2}\right) \quad (15)$$

$$U_{i+1/2}=\frac{2A}{n+1}\,[\tau_{i+1/2}]^n\left[\frac{H_{i+1}+H_i}{2}\right]\cos\alpha_{i+1/2} \quad (16)$$

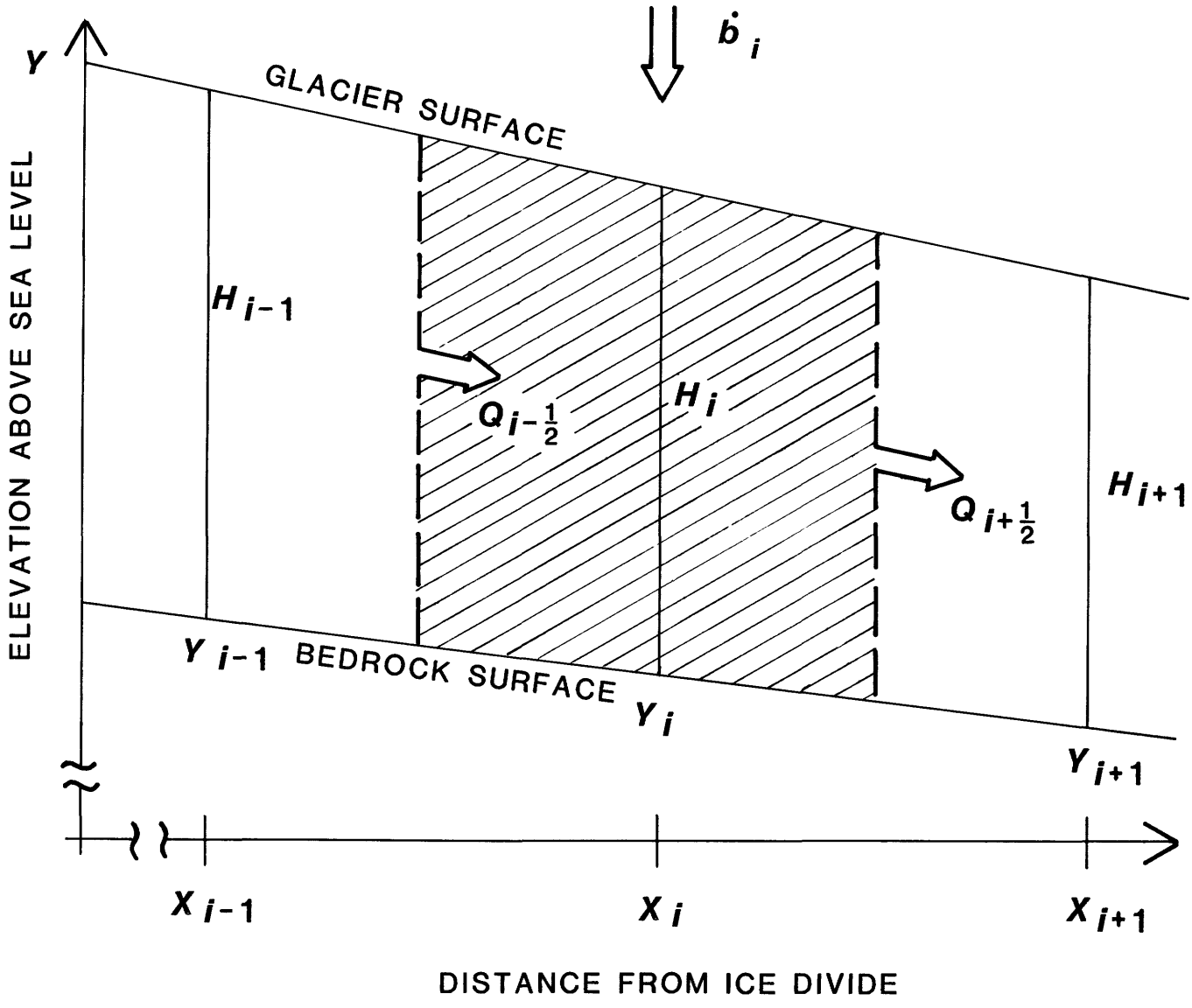

FIGURE 2. Schematic of finite-difference approximation of a longitudinal section of a glacier. Glacier is represented by a bedrock elevation, Y_i, and ice thickness, H_i, at each gridpoint, x_i. Continuity equation at x_i is applied over the hachured region with mass balance, $\dot{b}_i$, specified at x_i and volume fluxes, $Q_{i-1/2}$ and $Q_{i+1/1}$, calculated between x_{i-1}, x_i, and x_{i+1}.

$$\tau_{i+1/2}=f_{i+1/2}\left\{\frac{\phi}{x_{k+1}-x_h}\sum_{j=h}^{k}[\tau^*_{j+1/2}(x_{j+1}-x_j)]+(1-\phi)\tau^*_{i+1/2}\right\} \quad (17)$$

$$\tau^*_{i+1/2}=\varrho g\left[\frac{H_{i+1}+H_i}{2}\right]\sin\alpha_{i+1/2} \quad (18)$$

$$\alpha_{i+1/2}=\tan^{-1}\left[\frac{(H_i+Y_i)-(H_{i+1}+Y_{i+1})}{x_{i+1}-x_i}\right], \quad (19)$$

where $x_{k+1}-x_h$ is the large-scale averaging distance centered at $x_{i+1/2}$. As $x_{i+1/2}$ approached either end of the grid, the averaging distance necessarily decreased but remained centered on $x_{i+1/2}$.

BOUNDARY CONDITIONS

Equations 11 through 19 represent a second-order system; thus, their solution requires two boundary conditions. The scheme used in the Columbia Glacier calculations was to specify volume fluxes at the upstream and downstream ends of the modeled region. At the upstream boundary, a constant flux, $Q_{1/2}$, was specified that was approximately equal to the observed flux at this boundary. The use of this boundary condition assumes that the glacier behavior upstream of the boundary is unaffected by the response within the modeled region. For the modeling of Columbia Glacier,

this is probably a reasonable assumption over the short term (5–10 years) but limits the accuracy of predictions made over longer time scales.

At the downstream boundary, the terminus, a condition of constant flux is unreasonable. This is the most active region of the glacier during a retreat, so a boundary condition must be established that links this downstream volume flux to the glacier geometry. The method used to satisfy this second condition is to calculate a volume flux at the last gridpoint along the flowline and to use a backward-difference approximation for the flux gradient term in equation 11:

$$\frac{S_p^{m+1}-S_p^m}{t^{m+1}-t^m}+\frac{Q_p^{m+1/2}-Q_{p-1/2}^{m+1/2}}{\frac{1}{2}(x_p-x_{p-1})}=\dot{b}_p\ W_p, \qquad (11^*)$$

where x_p is the terminus gridpoint (fig. 3). The other modified equations are

$$Q_p=[f_p^*+\frac{\lambda_p}{1-\lambda_p}]U_p\ S_p \qquad (15^*)$$

$$U_p=\frac{2A}{n+1}\tau_p^n\ H_p\cos\alpha_p \qquad (16^*)$$

$$\tau_p=f_p\varrho g H_p\sin\alpha_p \qquad (17^*)$$

$$\alpha_p=\alpha_{p-1/2}. \qquad (19^*)$$

No large-scale average of τ^* is used in equation 17* because at the endpoints of the grid any centered large-scale average reduces to an average over the two gridpoints nearest the boundary.

This system of equations can be solved for the glacier depths at any time, given the geometry at any earlier time. Because the Crank-Nicholson approximation is implicit (that is, the H_i^{m+1} cannot be solved for directly), an iterative scheme was employed to converge to the unknown H_i^{m+1} at each time step. A Newston-Raphson technique was used, McCracken and Dorn (1964) give a general description of the method, and Bindschadler (1978) details its implementation in this model.

TEMPORAL BEHAVIOR OF TERMINUS

ADVANCE OR RETREAT

As mentioned earlier, the central issue in predicting the behavior of Columbia Glacier is predicting the time-dependent position of the terminus and the rate of calving. To calculate the new position of the terminus, once again, continuity is invoked, this time within the final segment of the glacier represented by the volume between the terminus positions at the beginning and end of any time step, $\triangle t$ (fig. 3). The volume of this segment is

$$M=(Q_p-\widetilde{Q})\triangle t, \qquad (20)$$

where $\widetilde{Q}$ is the calving flux (discussed below). The surface slope from x_{p-1} to x_p is assumed for any ice advancing beyond x_p, and the advance of the terminus calculated as

$$\delta=\frac{1}{\beta}\left\{\left[H_p^2+\frac{2(Q_p-\widetilde{Q})\triangle t\beta}{W_p}\right]^{1/2}-H_p\right\}, \qquad (21)$$

where $\beta=\frac{H_p-H_{p-1}}{x_p-x_{p-1}}$.

Equation 21 assumes a parallel-sided section of advancing or retreating ice with length δ and width W_p; within the nearest few hundred meters behind the shoal, the parallel-sided assumption is reasonable. The quantity δ is positive for an advance and negative for a retreat. The last gridpoint is then moved to the new terminus position, X_p^*, where the new ice depth is

$$H_p^*=H_p-\delta\frac{H_{p-1}-H_p}{x_p-x_{p-1}}. \qquad (22)$$

CALVING RELATIONSHIP

Equations 20 and 21 require that the flux of ice calving from the terminus, $\widetilde{Q}$, be known. The development of this relationship is the subject of a separate paper in this series on Columbia Glacier research (Brown and others, 1983). In summary, based on data from 13 temperate calving glaciers, the calving relationship that provides the best empirical fit to the data is

$$\widetilde{V}=ch_w, \qquad (23)$$

where $\widetilde{V}$ is the calving speed, h_w is the water depth at the center of channel, and c is a constant. Equation 23 will be referred to as the "water law." The best fit, providing a 0.84 coefficient of determination, is for $c=16.94\ a^{-1}$. As established by Post (1975), an irreversible, rapid retreat ensues when the terminus of a calving glacier enters deep water behind its shoal. An alternative formulation of calving speed, but with a smaller coefficient of determination, is

$$\widetilde{V}=c'H_p, \qquad (24)$$

where H_p is the ice thickness at the terminus instead of the water thickness. Equation 24 will be referred to as the "ice law." For either law of calving, the corresponding calving flux is

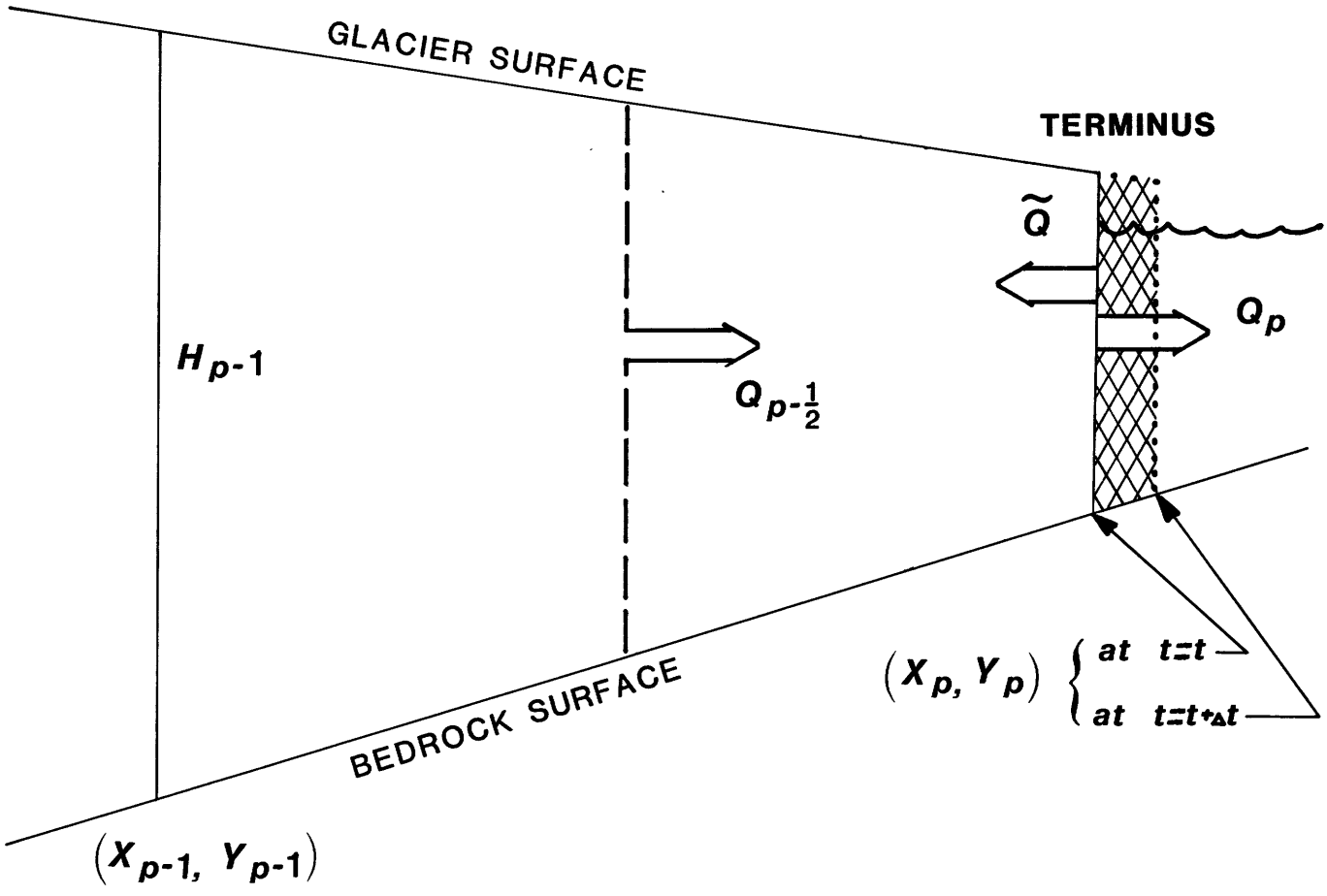

FIGURE 3. Schematic depicting modeled representation of calving terminus. Volume flux, Q_p, is calculated as described in text, and continuity equation applied at terminus is determined from calving flux ($\tilde{Q}$), Q_p, and continuity as described in text.

$$\tilde{Q}=\tilde{V}\,S_p. \tag{25}$$

Clearly equation 25 does not account for the strong seasonal variations in calving that have been measured on Columbia Glacier (Sikonia and Post, 1979); it quantifies the mean calving flux for a grounded terminus.

PREVENTION OF FLOATING TERMINUS

Although much of the physics involved in the calving process remains a mystery, there are still some physical constraints which can be incorporated into the model. The absence of any temperate ice shelves in the world strongly suggests that floating temperate ice quickly disaggregates into icebergs. This phenomenon was not incorporated into the empirical determination of the calving relationships (eqs 23, 24) because none of the tidewater glaciers studied had a floating or near-floating terminus. Nevertheless, the model's treatment of the motion of the terminus must be modified to take account of an expected dramatic increase in calving when the terminus is near flotation. Two alternative treatments were included in the model. The first was to locate the new terminus just upstream of any floating ice and to remove the floating ice from the glacier. This appeared rather arbitrary, however, and ignored the possible dynamic effects as the terminus approaches flotation.

A second, more involved, method was to modify the water law (eq 23) as follows:

$$\tilde{V}=\left[1+\frac{\theta}{1-\frac{\varrho_w\,h_w}{\varrho H_p}}\right] c\,h_w, \tag{26}$$

where H_p and h_w are the ice and water thicknesses, respectively, at the terminus; ϱ_w is the density of water at the terminus; and ϱ is a parameter that determines how sensitive calving is to a near-floating situation. For $\theta=0$, the calving speed is independent of buoyant

forces, and equation 26 reduces to the water law. To avoid a sudden transition to a floating terminus, the parameter θ had to be set to some small positive value, but no data were known to exist which might be used to estimate a reasonable value for θ.

Equation 26 does not ensure that at the end of a given time step there would not be some floating section of ice at the terminus. For larger values of θ, a floating situation was less likely to occur (a fact that possibly can be used as an ad hoc guide to reasonable values of θ), but the model still needed to be equipped to deal with this eventuality of floating ice within the final segment of the glacier. Rather than remove any floating volume of ice remaining at the end of a time step, it was redistributed over the surface of the final glacier segment (fig. 3). It was assumed that this redistribution was accomplished by some unprescribed dynamics during the most recent time step. By redistributing this extra mass in the shape of a wedge, the thickness at the gridpoint adjacent to the terminus remained unchanged, and a reduced surface slope compensated for the increased thickness at the terminus. This scheme rarely needed to be used and then resulted in only slight changes to the volume flux at the terminus. These special features of this particular mass redistribution maintained a relatively smooth behavior of the dynamic response of the glacier in the terminus area.

SUMMARY OF VARIABLES AND PARAMETERS

In the description of the model, numerous variables and parameters have been specified as necessary inputs to the model. They can be classified into the following groups: geometric, physical, and dynamic. In the geometric class are included the arrays of gridpoints, x_i; bed elevation, Y_i; ice thickness, H_i; and transverse channel shape, P_i and R_i (eqs 1, 2). The physical parameters include the constants of gravitational acceleration, g=9.8 m s^{-2}; ice density, ϱ=910 kg m^{-3}; and the ice-flow law parameters, n and A (eq 7). More generally, A is a function of ice temperature, ice fabric, and even impurity and water content. The final class includes the mass balance, $\dot{b}_i$ at each gridpoint; the velocity shape factors, $f_{i+1/2}$; flux shape factors, $f^*_{i+1/2}$; and sliding ratios, $\lambda_{i+1/2}$ specified at the midpoints of the grid. Also included in this class of dynamic parameters are the constants of upstream volume flux, $Q_{1/2}$; calving flux coefficient, c; averaging length, $x_k - x_h$; and weighting factor, ϕ (eq 6). With these parameters and variables chosen to represent the geometry and dynamics of a given glacier, the model predicts the future behavior of the glacier. The accuracy of the prediction rests on how precise the parameterization can be made and on the assumption that all of the important physical processes have been incorporated.

COLUMBIA GLACIER DATA

The model is general and may be applied to any glacier. What must be done for prediction of the time-dependent behavior of Columbia Glacier is to choose the appropriate parameter values that will yield the most accurate model representation of Columbia Glacier and that will serve as an initial condition. The field data used were collected primarily during the mass balance year from September 1, 1977, through August 31, 1978 (Mayo and others, 1979).

Figure 1 shows the complex, dendritic structure of the tributary glaciers, all of which contribute ice to the calving terminus. Modeling the entire glacier system would be a difficult task for the numerical models available and would require considerable data adjustment to provide a smooth initial condition. Thus, this model concentrated on the lower trunk of Columbia Glacier, the final 14 km (fig. 1). This permitted a finer grid resolution and a more accurate prediction of the sequence of events just prior to and during the initial rapid retreat phase. The assumption of only minor influence of the glacier upstream of the modeled region on the terminus behavior is justified by the expected imminence of rapid retreat. The surface topography and spatial distributions of surface velocity, mass balance, thickness change, and bed topography resulting from the field program are given by Sikonia (1983), Fountain (1982), and Mayo and others (1979). Because the present model does not account for seasonal variations, annually averaged data are used; the middle of the principal data year is 1978.2, at which time the transversely averaged position of the terminus was $X=x_{19}$=66.60 km, as measured from the head of the main trunk glacier.

The parameters must be chosen so that the initial conditions are consistent with the observed data as well as internally consistent with respect to each of the equations used to describe the glacier's dynamic behavior. Otherwise, the model would rapidly redistribute the mass of the glacier, not as a realistic projection of the glacier's future behavior, but artifically, to reconcile the inconsistencies in the initial conditions. Because there are numerous sources of uncertainty, both in the equations and in the observed data, the parameterization and construction of initial conditions is an underdetermined problem.

Uncertainties in the equations arise from such sources as the approximation of a three-dimensional flow regime by using a one-dimensional formulation with shape-factors parameterizing the effect of the

glacier channel on the longitudinal flow (eqs 13–15, 17); the representation of the longitudinal stresses by the slope-averaging scheme (eq 17); the assumption that the sliding component of motion follows the same functional form as the deformation component (eq 9); the treatment at the terminus of the calving mechanism (eqs 20–26); and the selection of particular numerical values for the flow law parameters (eq 7).

Uncertainties in the data include the bed topography, the spatial and temporal distributions of the fraction of the total velocity that is due to sliding, and the transverse averaging of the mass balance and the thickness change data, as well as the original observation error in all of the field data.

The underdeterminedness could be exploited by taking some of the variables to be determined exactly by the field data and then using the equations to calculate values for the other variables, but this could lead to unsatisfactory results. It could lead to values for the geometric or dynamic variables that might differ markedly from the field data. It could lead to values for the shape factors that might fictitiously represent features that could not be independently substantiated.

Instead, an error band was associated with the longitudinal profile of each variable, narrower for better-known variables, such as the surface elevation profile, and wider for less well-known variables, such as the bed profile. Then the profiles, beginning with the best estimates from the field data, were simultaneously adjusted, each within its own error band, so that they were smooth and free from extraneous features and were consistent through each of the equations.

A grid was established within 19 gridpoints equally spaced at intervals of 762.5 m. These gridpoints remained fixed in space with the exception of the last gridpoint, which moved with the terminus, as described in the previous section. The flow law parameters (eq 7) were set at $A=0.14$ bar^{-n} a^{-1} and $n=3$. These values for A and n, although not the result of any individual rheological study of ice (for example, Glen, 1955, or Nye, 1953), are typical of the values for temperate ice that have appeared in the literature. Any variation of A due to inhomogeneities of ice fabric or impurities is probably negligible. Figure 4 shows the adjusted profiles of the variables and represents a "best-fit" case. The lack of major features in the profiles is a result of the underdeterminedness of the fitting procedure.

One of the most important parameters remained outside this fitting procedure, the coefficient in either calving relationship (eqs 23, 24). The models of Rasmussen and Meier (1982) and especially Sikonia (1982) showed a marked sensitivity of the timing of rapid retreat to the calving relationship used. Thus, in the simulations that follow for this model, the sensitivity of the predictions to the value of this coefficient is keen interest.

PREDICTION OF COLUMBIA GLACIER BEHAVIOR

For any prediction computer run, a calving relationship (eqs 23, 24, 26) had to be specified with the appropriate parameters (c, c', or c and θ), and a method identified for treatment of floating ice (bulk removal or wedge redistribution). Thus, a large number of computer runs were possible. The approach taken here was first to examine the predicted response of the terminus for the water and ice laws of calving without any treatment for floating ice, then to use the modified water law with both treatments for floating ice, and finally to compare these predictions to available data of terminus position and suggest a "most-probable" scenario for the future behavior of Columbia Glacier.

WATER LAW VERSUS ICE LAW

In using either law, the value of the coefficient must be determined. This is accomplished by specifying an initial retreat rate and, from the known geometry and terminus volume flux (Q_p), by solving equation 20 for c (water law) or c' (ice law). Table 1 gives the coefficient values for various initial retreat rates.

The predicted response of the terminus for the five cases of table 1 are shown in figure 5. In each case, the rate of retreat slows from the initial value with the more pronounced decelerations for the ice law. Analysis of terminus position data completed after this modeling study indicated that retreat rates of 800 m a^{-1} were typical for the maximum retreat rate period during midsummer to late fall; however, Rasmussen and Meier (1982) calculate the average retreat rate during the 1977–78 measurement year to be 47 m a^{-1}. Figure 5 shows that the case W_1(c=16.934 a^{-1}, very close to the preferred value of 16.94 a^{-1} in eq 23) predicts an average retreat of 47 m in the first year. This result lends credence to this particular choice of water law and c in

TABLE 1.—Initial retreat rates for various values of coefficient in water and ice calving laws

Law	Initial retreat rate		
	200 m a^{-1}	400 m a^{-1}	800 m a^{-1}
Water: c	14.739 a^{-1}	16.934 a^{-1}	20.000 a^{-1}
Ice: c'	8.817 a^{-1}	10.130 a^{-1}	—

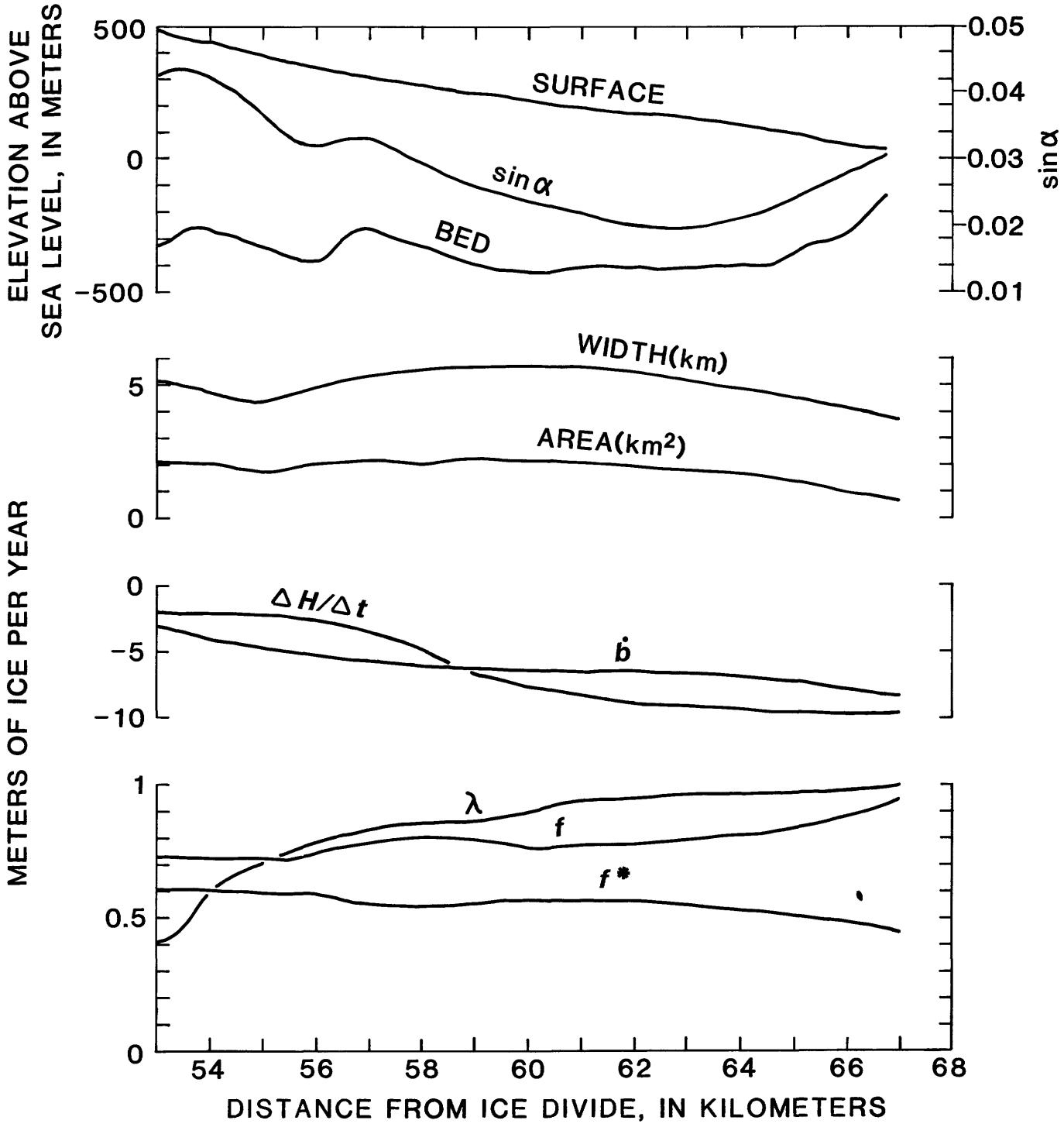

FIGURE 4. Longitudinal profiles of important variables for Columbia Glacier. Distances are measured from ice divide of main trunk glacier (fig. 1).

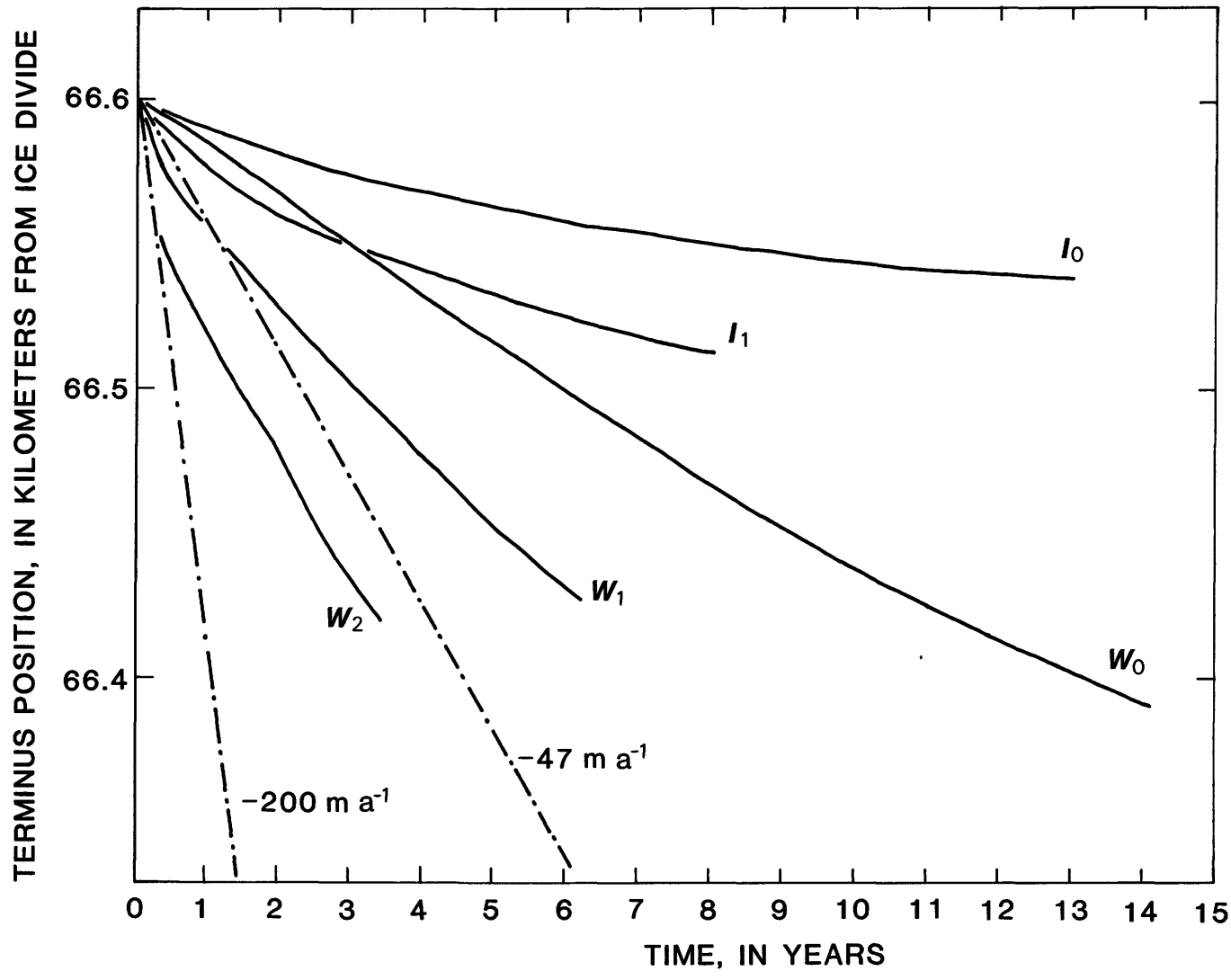

FIGURE 5. Predictions of terminus retreat for various calving parameterizations. Curves labeled I_0 and I_1 correspond to ice law of calving (eq 24) with c'=8.817 a^{-1} for I_0 and 10.130 a^{-1} for I_1. Curves labeled W_0, W_1, and W_2 correspond to water law of calving (eq 23) with c=14.739, 16.900, and 20.000 a^{-1}, respectively.

the model and to the effective parameterization of the glacier dynamics by showing that the predicted retreat rates are controlled more by the dynamics of the glacier than by the initial retreat rate used.

EFFECT OF FLOATING ICE

The predictions of any of the curves in figure 5 are not reliable once the ice thickness at the terminus is near to the flotation thickness. Figure 6 illustrates how the behavior of the terminus is changed when the modified water law (eq 26) is used for various values of c and θ and an initial retreat rate of 400 m a^{-1}. The curve labeled "Flotation ignored" corresponds to curve W_1 in figure 5. In every case where flotation was parameterized, the glacier progresses into a phase of very rapid retreat. This retreat could only be followed for a few hundred meters because, as the retreat accelerated, the computation time step shrank to a few minutes which lengthened the required computing time prohibitively.

Figure 6 also shows that for θ=0, the wedge redistribution of floating ice delays the timing of the drastic retreat from the case when the floating ice is removed. The delay, however, only amounts to a few months. The rapid retreat is dramatic because, once the terminus retreats into deeper water, so much of the ice is near the flotation thickness; continued thinning near the terminus causes increasingly larger volumes of ice to float.

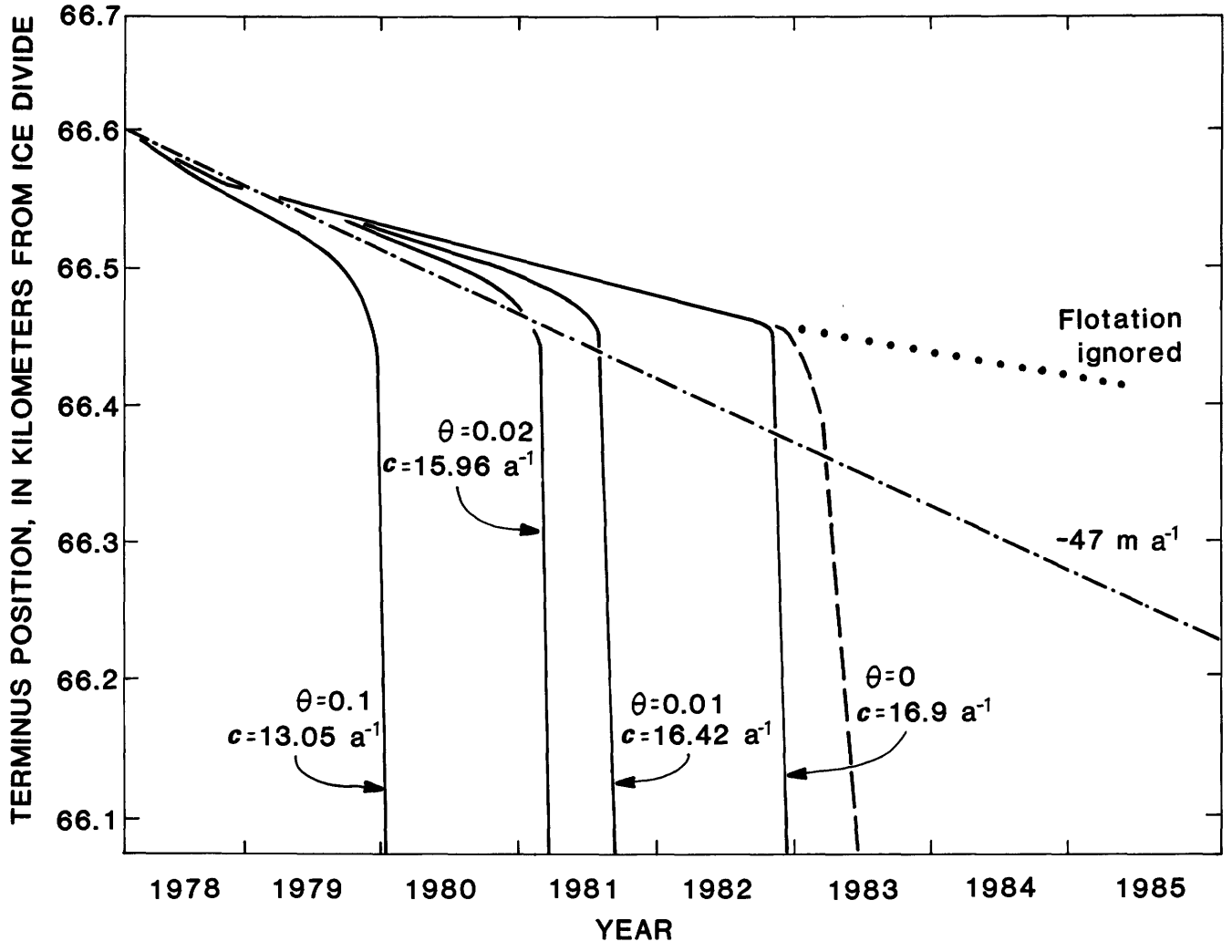

FIGURE 6. Predicted terminus retreat using modified water law of calving (eq 26) for various values of c and θ. Each case refers to an initial terminus retreat of 400 m a^{-1}. Dotted curve results from ignoring flotation (see curve W_1, fig. 5); dashed curve results from a wedge redistribution scheme for floating ice; and all others result from removing any floating ice from terminus.

The other curves in figure 6 complete a consistent picture of the effect of different values for θ on the timing of the rapid retreat. The general results are that the onset of rapid retreat occurs sooner, and, as θ increases, the transition to rapid retreat is smoother. In each run with a different θ value, the value of c was adjusted to preserve the same initial retreat of 400 m a^{-1}.

An even more significant result is that, despite the variation in *when* the rapid retreat begins, the position of the terminus at that time is roughly the same in all of the cases shown. This suggests that even if the most reasonable value of θ is not well known, the onset of the rapid retreat of Columbia Glacier might still be predicted by monitoring the position of the terminus.

When the time axis is expressed as calendar dates (fig. 6), t=0 corresponds to 1978.2 as this is the approximate midpoint of the 1977–78 balance year during which most of the field data were collected. By including this dateline in figure 6, it can be seen that, if the model is valid, θ must be very small because by late 1981 the rapid retreat phase had not yet been observed.

COMPARISON OF PREDICTION WITH OBSERVED RETREAT

Figure 7 compares the observational time series of width-averaged terminus positions with many runs of the model using the water law for calving (c=14.74, 16.90, and 20.00 a^{-1}) and each alternative for treating floating ice (no adjustment, bulk removal, and wedge redistribution). Based on figures 5 and 6, the case of c=16.9 a^{-1} and a wedge redistribution appears to be the most realistic parameterization, and, indeed, figure 7 shows that the predictions for this case generally fit quite well within the observed seasonal fluctations of

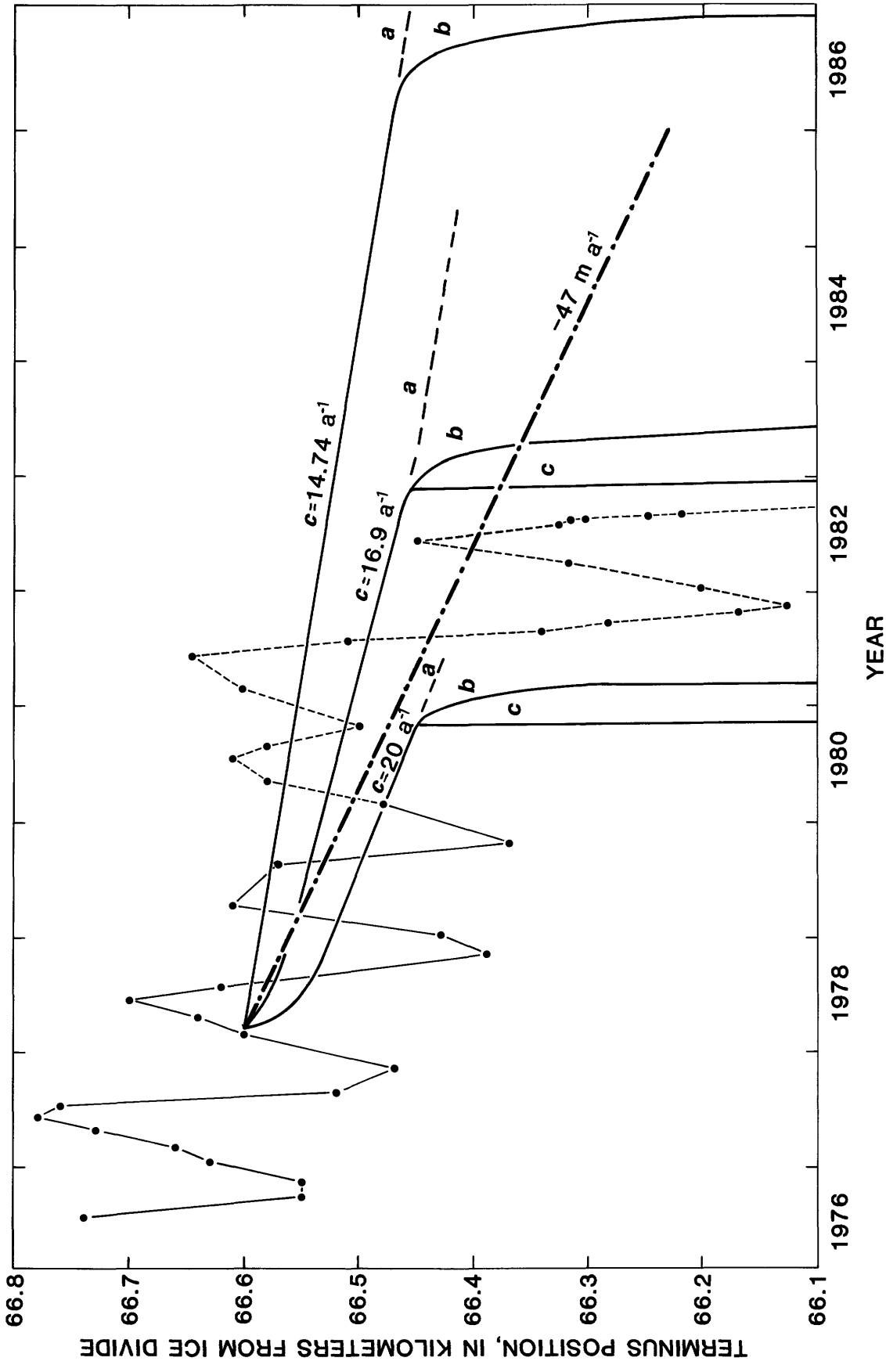

FIGURE 7. Predicted terminus retreat with modified water law of calving (eq 26 wherein $\theta=0$) for various treatments of floating ice and values of c as follows: a, no flotation condition; b, wedge redistribution of floating ice; and c, removal of floating ice. Also shown are data of observed terminus position: solid line preceded model study, dotted line postdated completion of model study, and dots indicate measured values.

terminus position. Data confirmed that the retreat in fall 1980 was truncated by an abnormally cold and snowy August and that the pronounced retreat in summer 1981 finally ended in November when a readvance began (M. F. Meier, personal commun., 1981). Comparing those data to figure 6, it can be seen that the retreat measured in 1981 fits the case of $c=16.9$ a^{-1} and $\theta=0.01$ well, except that in the model no recovery was possible.

Also from figure 7, it is clear that $c=20.00$ a^{-1} is too high a value and that $c=14.74$ a^{-1} is too low for the coefficient of the water law of calving. Again, although the time of onset of rapid retreat is sensitive to the value of c, the terminus position at that time falls within a relatively narrow range. This result might have significance in understanding more about the dynamics of rapid retreat but would be difficult to use in practice due to the large seasonal fluctuation of terminus position and its variability across the terminus width when large embayments are present.

The predicted rate of thinning over the lower glacier for the preferred case $c=16.9$ a^{-1}, $\theta=0$ is shown in figure 8 up to the moment of drastic retreat. The rate of thinning at the terminus decreases slightly until flotation is approached. Observations indicate that the recent thinning which has occurred over the lower section of Columbia Glacier has been more uniform spatially than figure 8 indicates and that this thinning has been proceeding at an average rate of about 3.5 m a^{-1} (M. F. Meier, personal commun., 1982). This might be due to the role of longitudinal stresses in the dynamics in this region or to a temporal change in the propor-

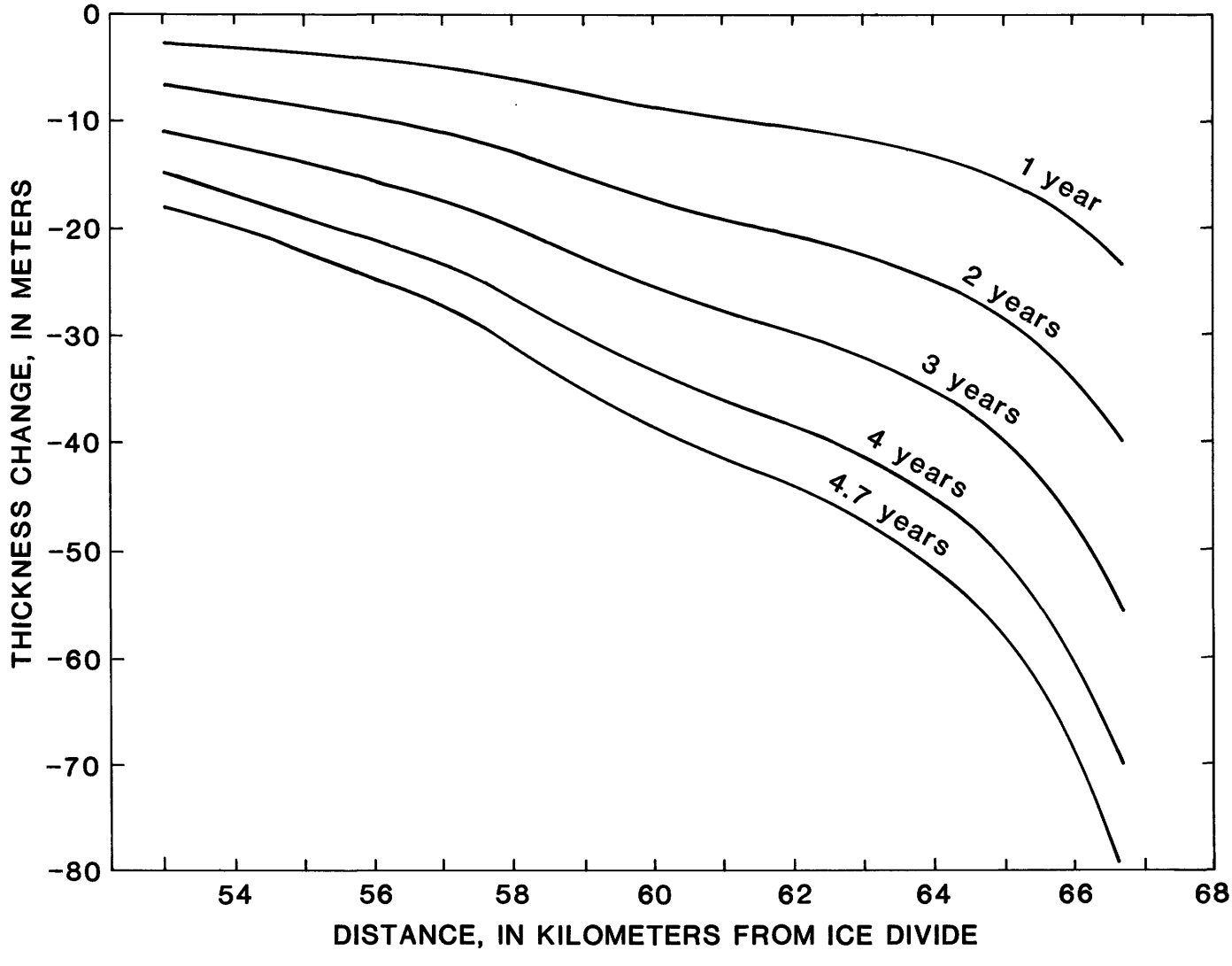

FIGURE 8. Profiles of predicted thickness change since 1978.2 for $c=16.9$ a^{-1} and $\theta=0$. At 4.7 years (or date 1982.9), flotation occurs at the terminus and rapid retreat begins.

tional contribution of sliding velocity, neither of which are explicity included in the model. In the model, the longitudinal gradient of thinning represents the glacier's adjustment to accommodate an increasing calving flux. With time, the surface slope of the glacier steepens to provide more mass at the terminus, but the required thinning is so extreme that approach to flotation and rapid retreat are unavoidable. If the volume flux at the terminus could be increased without increasing the surface slope, then flotation might not precede rapid retreat. An example of this might be if the sliding velocity were to increase. If this were the case, thinning would be more widespread and uniform but would decrease the ability of the glacier to increase the volume flux later. This process appears to be important in the Sikonia (1982) finite-element model when rapid retreat is predicted. In either case, because the increase of calving flux is so rapid for even a slight retreat (owing to the steep slope of the shoal on the up-glacier side), the glacier must be able to respond quickly with a much-increased flux of ice to the terminus. If it cannot, then the retreat will quickly become irreversible.

Additional evidence that flotation may play an important role in rapid retreat can be drawn from studies of the embayments which have formed annually at the terminus in recent years (Sikonia and Post, 1979). The location of these embayments usually coincides with the position of the major subglacial drainage channel (Sikonia and Post, 1979). The pressure of the water in this channel has been calculated to be large enough to float the ice locally (Bindschadler, 1982) causing a localized catastrophic retreat which is impeded only by the stability of the surrounding ice. These embayments have been observed to form very quickly. Their size has increased annually, presumably because the terminus is thinner and, as a whole, is less able to retard the formation of expanding embayments.

The finite-difference model, however, cannot model this embayment behavior because the growth is caused by seasonal increases in the calving flux and their extent is limited by altered transverse stresses within the more stable surrounding ice. Nevertheless, the model predictions presented here suggest that Columbia Glacier will most likely begin an irreversible phase of very rapid retreat in the 1980's. This irreversible retreat will probably first manifest itself by a continued retreat during the winter months when the terminus has, heretofore, readvanced (fig. 7).

REFERENCES CITED

Bindschadler, R. A., 1978, A time-dependent model of temperate glacier flow and its application to predict changes in the surge-type Variegated Glacier during its quiescent phase: Unpublished thesis, University of Washington Geophysics Program, Seattle, Washington, 244 p.

———1982, A numerical model of temperate glacier flow applied to the quiescent phase of a surge-type glacier: Journal of Glaciology, v. 28, no. 99, p. 239–265.

———1983, The importance of pressurized sub-glacial water in separation and sliding at the glacier bed: Journal of Glaciology. (In press.)

Brown, C. S., Meier, M. F., and Post, Austin, 1982, The calving relation of Alaskan tidewater glaciers, with application to Columbia Glacier: U.S. Geological Survey Professional Paper 1258–C, 13 p.

Budd., W. F., 1970, The longitudinal stress and strain-rate gradients in ice masses: Journal of Glaciology, v. 9, no. 55, p. 19–27.

Fountain, A. G., 1982, Columbia Glacier Photogrammetric Altitude and Velocity: Data Set (1957–1981), U.S. Geological Survey Open-File Report 82–756, 225 p.

Glen, J. W., 1955, The creep of polycrystalline ice: Proceedings of the Royal Society, Series A, v. 228, p. 519–538.

Iken, Almut, 1981, The effect of the sub-glacial water pressure on the sliding velocity of a glacier in an idealized numerical model: Journal of Glaciology, v. 27, no. 97, p. 407–421.

Kamb, Barclay, 1970, Sliding motion of glaciers—Theory and observation: Reviews of Geophysics and Space Physics, v. 8, no. 4, p. 673–728.

Kollmeyer, R. C., Motherway, D. L., Robe, R. Q., Platz, B. W., and Shah, A. M., 1977, A design feasibility study for the containment of icebergs within the waters of Columbia Bay, Alaska: U.S. Coast Guard Final Report No. 128, 135 p.

Lliboutry, Louis, 1968, General theory of sub-glacial cavitation and sliding of temperate glaciers: Journal of Glaciology, v. 7, no. 49, p. 21–58.

Mayo, L. R., Trabant, D. C., March, Rod., and Haeberli, W., 1979, Columbia Glacier stake location, mass balance, glacier surface altitude, and ice radar data, 1978 measurement year: U.S. Geological Survey Open-File Report 79–1168, 72 p.

McCracken, D. D. and Dorn, W. S., 1964, Numerical methods and FORTRAN programming: John Wiley & Sons, Inc., New York, 455 p.

Meier, M. F., 1968, Calculations of slip of Nisqually Glacier on its bed: No simple relation of sliding velocity to shear stress: Union de Geodesie et Geophysique Internationale, Association Internationale d'Hydrologie Scienfitique, Assemblee generale de Berne, 1967, Commission de Neiges et Glaces, Rapports et discussions, p. 49–57.

Meier, M. F., Kamb, Barclay, Allen, C. R., Sharp, R. T., 1974, Flow of Blue Glacier, Olympic Mountains, Washington, U.S.A.: Journal of Glaciology, v. 13, no. 68, p. 187–212.

Meier, M. F., Post, Austin, Brown, C. S., Frank, David, Hodge, S. M., Mayo, L. R., Rasmussen, L. A., Senear, E. A., Sikonia, W. G., Trabant, D. C., and Watts, R. D., 1978, Columbia Glacier progress report—December 1977: U.S. Geological Survey Open-File 78–264. 56 p.

Meier, M. F., Rasmussen, L. A., Post, Austin, Brown, C. S., Sikonia, W. G., Bindschadler, R. A., Mayo, L. R., and Trabant, D. C., 1980, Predicted timing and disintegration of the lower reach of Columbia Glacier, Alaska: U.S. Geological Survey Open-File Report 80–582, 47 p.

Morland, L. W., 1976a, Glacier flow down an inclined wavy bed: Journal of Glaciology, vo. 17, no. 77, p. 447–462.

———1976b,, Glacier flow down an inclined wavy bed with friction: Journal of Glaciology, v. 17, no. 77, p. 463–477.

Nye, J. F., 1953, The flow law of ice from measurements in glacier tunnels, laboratory experiments and the Jungfraufirn borehole

experiment: Proceedings of the Royal Society, Series A, v. 219, p. 477–489.

———1957, The distribution of stress and velocity in glaciers and ice sheets: Proceedings of the Royal Society of London, Series A, v. 239, p. 113–133.

———1965, The flow of a glacier in a channel of rectangular, elliptic, or parabolic cross-section: Journal of Glaciology, v. 5, no. 41, p. 661–690.

Post, Austin, 1975, Preliminary hydrography and historic terminal changes of Columbia Glacier, Alaska: U.S. Geological Survey Hydrologic Investigations Atlas 559, 3 sheets.

———1980a, Preliminary bathymetry of Northwestern Fiord and neoglacial changes of Northwestern Glacier, Alaska: U.S. Geological Survey Open-File Report 80–414, 2 sheets.

———1980b, Preliminary bathymetry of Blackstone Bay and neoglacial changes of Blackstone Glacier, Alaska: U.S. Geological Survey Open-File Report 80-418, 2 sheets.

———1980c, Preliminary bathymetry of Aialik Bay and neological changes of Aialik and Pederson Glaciers, Alaska: U.S. Geological Survey Open-File Report 80–423, 1 sheet.

———1980d, Preliminary bathymetry of McCarty Fiord and neoglacial changes of McCarty Glacier, Alaska: U.S. Geological Survey Open-File Report 80–424, 4 sheets.

———1980e, Preliminary bathymetry—Esther Passage to Eaglek Island, Alaska: U.S. Geological Survey Open-File Report 80–426, 1 sheet.

———1980f, Preliminary bathymetry—Approaches to Unakwik Inlet, Alaska: U.S. Geological Survey Open-File Report 80–428, 1 sheet.

Rasmussen, L. A., and Meier, M. F., 1982, Continuity equation model of the drastic retreat of Columbia Glacier, Alaska: U.S. Geological Survey Professional Paper 1258–A, 23 p.

Sikonia, W. G., and Post, Austin, 1979, Colu;mbia glacier, Alaska—Recent ice loss and its relationship to seasonal terminal embayments, thinning, and glacier flow: U.S. Geological Survey Open-File Report 79–1265, 2 sheets.

Sikonia, W. G., 1982, Finite element model of drastic retreat of Columbia Glacier, Alaska: U.S. Geological Survey Professional Paper 1258–B, 74 p.

———1983, Two-dimensional adjustment of point data, Columbia Glacier, Alaska: U.S. Geological Survey Open-File Report. (In press.)

Waddington, E. D., 1981, Accurate modelling of glacier flow: Unpublished thesis, The University of British Columbia, Vancouver, British Columbia, 460 p.

Weertman, Johannes, 1964, The theory of glacier sliding: Journal of Glaciology, vo. 5, no. 39, p. 287–303.